Experimental Study on Accurate Calibration for Industrial Robot Via Integrated Extended Kalman and Beetle Antennae Search

Zhibin Li, Shuai Li, *Senior Member*, *IEEE*, and Xin Luo, *Senior Member*, *IEEE*

***Abstract*—**Over the past decades, industrial robots have been widely used in aerospace, electronics, medical and other fields. However, the absolute positioning error of uncalibrated robot can achieve several millimeters, which cannot meet the accuracy requirements of advanced industry. To address this issue, it is necessary to calibrate the robot. Therefore, based on the DH model，a new robot calibration method combining the extended Kalman filter with quadratic interpolation beetle antennae search algorithm is proposed. Firstly, the DH model of the robot is built. Then the extended Kalman filter is adopted to preliminarily identify the robot kinematic parameters to address the issue of non-Gauss noises. Meanwhile, quadratic interpolation beetle antennae search algorithm is adopted to further calibrate the kinematic parameters. Lastly, extensive experiments are carried out on an ABB IRB 120 industrial robot. The experimental results show that the robot positioning error is significantly reduced by the proposed algorithm, which is appropriate for practical application occasions with high-precision requirements.

***Index Terms*—**Extended Kalman Filter (EKF), Quadratic Interpolation Beetle Antennae Search (QIBAS), Non-Gauss Noises, Kinematic Parameters, Absolute Positioning Error.

I. INTRODUCTION

INDUSTRIAL robots achieve a rapid development in the Industry 4.0, which have been widely adopted in intelligent manufacture, intelligent life, intelligent medicine and other advanced fields [1-5]. Meanwhile, they also play a vital role in achieving industrial automation [5-10].

Industrial robots are the core equipment of industrial production and application, which need to meet the higher technical requirements of the developing complex industry. Commonly, the robot has high repetitive positioning accuracy, but the absolute positioning accuracy is low. There are numerous factors affecting the absolute positioning accuracy of robot, which can be divided into non-geometric error and geometric error. Among them, the geometric error of robot accounts for about 90% of total error sources. The geometric error contains assembly error, manufacturing tolerance, structural deformation, which eventually leads to the robot positioning error. Thus, it is necessary to calibrate the robot and identify the actual kinematic parameters.

To address the issue of low absolute positioning accuracy of robot, researchers have conducted extensive research [12-15]. They have proposed numerous intelligent algorithms to identify the kinematic parameters, like Levenberg-Marquardt (LM) algorithm, EKF algorithm, particle filter (PF) algorithm, genetic algorithm (GA) and neural networks. Luo *et al*. [1] propose a calibration method based on LM and differential evolution hybrid algorithm to estimate the kinematic parameter deviations. Then, enough experiments are conducted on an industrial robot FANUC M710ic/50. After calibration, this method obtains a greatly improvement on the robot calibration accuracy. Wang *et al*. [2] develop a new algorithm combining back propagation neural network and analytical method to calibrate the robot, which considers geometric error, external load, etc. They achieve excellent experimental results on an ABB IRB 6640 industrial robot. Zhong *et al*. [3] adopt the improved whale swarm algorithm to calibrate the legged robots with a constraint handling mechanism, which successfully identifies the kinematic parameters. In general, these algorithms can improve the robot calibration accuracy. However, these algorithms have slow convergence rate and easily fall into the local optimum. Meanwhile, the experimental code is highly complex, which also can not deal with the non-Gaussian noises.

In general, metaheuristic algorithms are based on the rule of computational intelligence [11-16], which are adopted to overcome the complex optimization issues. The commonly used metaheuristic algorithms contain differential evolution algorithm (DE) [17], iterated greedy algorithm (IG), particle swarm optimization algorithm (PSO) [14] and ant colony optimization algorithm (ACO). The proposed QIBAS algorithm is one of metaheuristic algorithms, which simulates foraging principle of a beetle. It only requires one individual to complete the optimization process, thus the search process is greatly fast. Furthermore, it has the advantages of simple principle, minimal computing resources, strong search ability.

For the above-mentioned shortcomings of these algorithms,

✧ This research is supported by the National Natural Science Foundation of China under grant 62272078, and the CAAI-Huawei MindSpore Open Fund under Grant CAAIXSJLJJ-2021-035A. (Corresponding authors: X. Luo and S. Li).

✧ Z. Li is with the School of Computer Science and Technology, Chongqing University of Posts and Telecommunications, Chongqing 400065, China, and also with the Chongqing Institute of Green and Intelligent Technology, Chinese Academy of Sciences, and also with the Chongqing School, University of Chinese Academy of Sciences, Chongqing 400714, China (e-mail: LiZhibin111@outlook.com).

✧ S. Li is with the Faculty of Information Technology and Electrical Engineering, University of Oulu, Pentti Kaiteran katu 1, Oulu, Finland (email: sliuoulu@gmail.com).

✧ X. Luo is with the College of Computer and Information Science, Southwest University, Chongqing 400715, China (email: luoxin@swu.edu.cn).

we develop a new calibration algorithm based on EKF and QIBAS algorithm. Firstly, we describe the kinematic model and error model of the robot. Considering the influence of non-Gaussian noises in the actual measurement process, EKF algorithm is used to initially identify the kinematic parameters.Then, QIBAS algorithm is adopted to further optimize the robot positioning error. Finally, enough experiments are conducted on an ABB IRB120 robot to verify the feasibility of the proposed method.

We adopt a new calibration algorithm based on EKF algorithm and QIBAS algorithm, which modifies learning rule of conventional beetle antennae search (BAS) algorithm to improve its search ability. Meanwhile, it also effectively overcomes the issue of non-Gauss noises. After calibration, the robot calibration accuracy is significantly improved. Moreover, the main contributions of this paper include:

a) We develop a QIBAS algorithm based on a BAS algorithm, which incorporates the quadratic interpolation operator into the updating rule of the standard BAS to achieve faster convergence rate and higher calibration accuracy than its peers do;
b) A novel calibration algorithm based on EKF algorithm and QIBAS algorithm is proposed to achieve the accurate identification of robot kinematic parameter errors;
c) Algorithm design are conducted for the proposed EKF-QIBAS approach as a guidance for scholars.

Extensively empirical results are conducted on an ABB IRB120 industrial robot, which demonstrates that the proposed calibration algorithm obtains much higher calibration accuracy than advanced calibration algorithms.

For the rest of this paper, Section II discusses the robot kinematic and error models. Section III briefly introduces the EKF and QIBAS algorithm. Section IV presents the experimental results and analyses. Lastly, Section V provides the conclusions and future work.

TABLE I
NOMINAL VALUES OF KINEMATIC PARAMETERS FOR ABB IRB 120 ROBOT.

Joint *i*	α_i/°	a_i/mm	d_i/mm	θ_i/°
1	-90	0	290	0
2	0	270	0	-90
3	-90	70	0	0
4	90	0	302	0
5	-90	0	0	0
6	0	0	72	0

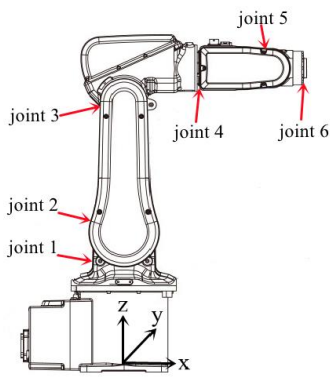

Fig. 1. The model of an ABB IRB120 industrial robot.

II. KINEMATIC AND ERROR MODELS FOR CALIBRATION

A. Kinematic Model

Commonly, the widely used kinematic models in robot controller contain DH model [4], [5], MDH model, POE model [8] and CPC model [14], [17]. The most commonly used kinematic model is the DH model proposed by Denavit and Hartenberg. The virtue of DH model is that the relative relationship between the robot end-effector and the base coordinate system can be expressed through the calculation relationship of the transformation matrix, which is convenient for solution. The structure of an ABB IRB 120 robot is depicted in Fig. 1, whose nominal values of robot kinematic parameters are listed in Table I.

Based on the DH model [9], [10], the transformation matrix from link i-1 to link i is as follow:

$$A_i = \begin{bmatrix} \cos\theta_i & -\sin\theta_i\cos\alpha_i & \sin\theta_i\sin\alpha_i & a_i\cos\theta_i \\ \sin\theta_i & \cos\theta_i\cos\alpha_i & -\cos\theta_i\sin\alpha_i & a_i\sin\theta_i \\ 0 & \sin\alpha_i & \cos\alpha_i & d_i \\ 0 & 0 & 0 & 1 \end{bmatrix}, \quad (1)$$

where A_i is the transformation matrix, a_i, d_i, θ_i and α_i denote link length, link offset, joint angle, link twist angle of the ith link, respectively. Thus, the robot kinematic model can be expressed as:

$$T_6 = A_1A_2A_3A_4A_5A_6 = \begin{bmatrix} R_N & P_N \\ 0 & 1 \end{bmatrix}, \quad (2)$$

where R_N, P_N are the nominal rotation matrix and the nominal position vector of the robot, respectively.

B. Error Model

Based on the link transformation matrices [15-20], the pose error of the robot end-effector can be expressed as:

$$dT = T_r - T_6, \quad (3)$$

where dT, T_r and T_6 represent the pose deviation, the actual pose of the end-effector and the nominal pose of the end-effector, respectively.

Additionally, the pose error model is calculated by:

$$\Delta E = \begin{bmatrix} H_1 & H_2 & H_3 & H_4 \end{bmatrix} \begin{bmatrix} \Delta a \\ \Delta d \\ \Delta\alpha \\ \Delta\theta \end{bmatrix} = H\Delta\eta, \quad (4)$$

where H, $\Delta\eta$ are the Jacobian matrix and DH parameters deviations, respectively.

According to the nominal cable length Y'_i and the measuring cable length Y_i, the objective function for optimizing robot positioning errors is as follow:

$$f = \min\left\|\Delta E\right\|_2^2 = \min\left[\frac{1}{n}\sum_{i=1}^{n}\left(Y_i - Y_i'\right)^2\right]. \quad (5)$$

Commonly, based on the robot end-effector position coordinate P_i and the fixed point coordinate P_0 on the ground, the nominal cable length is calculated by:

$$Y_i' = \sqrt{\left(P_i - P_0\right)^2}. \quad (6)$$

III. Robot Kinematic Parameter Identification Algorithm

A. EKF Algorithm

Due to the influence of measurement noises, the EKF algorithm is applied to estimate the robot position error [5]. Its state equation and output equation can be represented as:

$$\begin{aligned} \eta_{k|k-1} &= \eta_{k-1|k-1}, \\ Z_k &= H_k \eta_k + V_k, \end{aligned} \tag{7}$$

where η, Z_k, H and V_k are the DH parameters deviations, the measuring position error of end-effector, Jacobian matrix and measurement error, respectively. Moreover, the error covariance matrix P_k and the covariance matrix of the system noise Q_k are expressed as:

$$P_{k|k-1} = P_{k-1|k-1} + Q_{k-1}. \tag{8}$$

Based on (7) and (8), the Kalman gain K_k is as follow:

$$K_k = P_{k|k-1} H_k^T \left(H_k P_{k|k-1} H_k^T + R_k \right)^{-1}, \tag{9}$$

where R_k represents the covariance matrix, then the parameter η can be updated by

$$\eta_{k|k} = \eta_{k|k-1} + K_k \left(Z_k - H_k \eta_{k|k-1} \right). \tag{10}$$

Furthermore, the covariance matrix P is as follow:

$$P_{k|k} = \left(I - K_k H_k \right) P_{k|k-1}. \tag{11}$$

Generally, P, Q and R are initialized by $10^{-6}I$, $10^{-6}I$, and $10^{-4}I$, respectively.

B. QIBAS Algorithm

BAS algorithm is also one of metaheuristic algorithms, which is an intelligent optimization algorithm proposed by Jiang *et al* [10]. This method simulates the food searching behavior of a beetle, which has the advantages of strong search ability, less calculation parameters.

The decision parameters for BAS algorithm are as follow:

$$\eta = \left[\eta_1, \quad \eta_2, \quad \cdots \quad \eta_n \right]^T. \tag{12}$$

Based on the learning rule of BAS algorithm, we obtain that

$$\eta_{t+1} = \eta_t + \delta_t \vec{b} sign\left(f\left(\eta_{rt}\right) - f\left(\eta_{lt}\right) \right), \tag{13}$$

where δ, $\vec{b}$ and $sign(\cdot)$ are the step size of searching, a random searching direction and the sign function, respectively. Then we have

$$\vec{b} = \frac{rands(k,1)}{\left\| rands(k,1) \right\|_2}, \tag{14}$$

where rands is the random function, k is position dimension, $||\cdot||_2$ is L_2 norm. Thus, we obtain the searching behaviors of a beetle.

$$\begin{aligned} \eta_{rt} &= \eta_t + m_t \vec{b}, \\ \eta_{lt} &= \eta_t - m_t \vec{b}, \end{aligned} \tag{15}$$

where m is the antennae length. Then m and δ can be calculated by

$$\begin{aligned} \delta_{t+1} &= \mu \delta_t + \delta_0, \\ m_{t+1} &= \tau m_t + m_0, \end{aligned} \tag{16}$$

where $\mu \in (0,1)$, $\tau \in (0,1)$, $\delta_0 > 0$, $m_0 > 0$. δ is the step size of searching.

The search scope is defined in a closed set Φ, the BAS algorithm is rewritten as

$$\eta_{t+1} = P_\Phi \left(\eta_t + \delta_t \vec{b} sign\left(f\left(\eta_{rt}\right) - f\left(\eta_{lt}\right) \right) \right), \tag{17}$$

where $P_\Phi(\cdot)$ represents a projection operator, η has the bound $\Phi = \{\eta | l_i \le \eta_i \le \omega_i\}$. Then the lower bound $l = [l_1, l_2, \ldots, l_n]^T$ and the upper bound $\omega = [\omega_1, \omega_2, \ldots, \omega_n]^T$ can be obtained in this work. And finally, the $g = P_\Phi(\eta)$ is given as

$$g_i = \begin{cases} l_i, & if \ \ \eta_i < l_i, \\ \eta_i, & if \ \ l_i \le \eta_i \le \omega_i, \\ \omega_i, & if \ \ \eta_i > \omega_i. \end{cases} \tag{18}$$

Nevertheless, the BAS algorithm is easy to fall into local optimum, which results in the low search accuracy.

To overcome this issue, the quadratic interpolation operator is added into the BAS algorithm. It continuously adopts the quadratic polynomials to approximate the objective function in the search process. Therefore, the obtaining minimum of the simulated function is approximately equal to the minimum of the objective function [11-15].

The approximate expression of the objective function is defined as a second-order polynomial, we achieve that

$$h\left(\eta_i\right) = c_0 + c_1 \eta_i + c_2 \eta_i^2 = f\left(\eta_i\right), \tag{19}$$

where c_0, c_1, c_2 are constants. To achieve the stable equilibrium point of binomial $h(\eta_i)$, its first derivative is zero, then we have

$$h'\left(\eta_i\right) = c_1 + 2c_2 \eta_i = 0, \tag{20}$$

With (20), the stable equilibrium point is given as

$$\eta_{tk} = -\frac{c_1}{2c_2}. \tag{21}$$

In addition, the location of left and right tentacles, global optimal location are as follow:

$$\begin{aligned} \eta_l &= \left[\eta_{l1}, \quad \eta_{l2}, \quad \cdots, \quad \eta_{lk} \right]^T, \\ \eta_r &= \left[\eta_{r1}, \quad \eta_{r2}, \quad \cdots, \quad \eta_{rk} \right]^T, \\ \eta_b &= \left[\eta_{b1}, \quad \eta_{b2}, \quad \cdots, \quad \eta_{bk} \right]^T. \end{aligned} \tag{22}$$

With equation (22) and equation (19), then we actually can achieve that

$$\begin{cases} h\left(\eta_{lk}\right) = c_0 + c_1 \eta_{lk} + c_2 \eta_{lk}^2 = f\left(\eta_{lk}\right) = f_1, \\ h\left(\eta_{rk}\right) = c_0 + c_1 \eta_{rk} + c_2 \eta_{rk}^2 = f\left(\eta_{rk}\right) = f_2, \\ h\left(\eta_{bk}\right) = c_0 + c_1 \eta_{bk} + c_2 \eta_{bk}^2 = f\left(\eta_{bk}\right) = f_3, \end{cases} \tag{23}$$

where $k = 1, 2, \cdots, n$, $\chi_1 = \eta_{lk}$, $\chi_2 = \eta_{rk}$, $\chi_3 = \eta_{bk}$, $\chi = \eta_{tk}$.

$$\chi = \frac{\left(\chi_1^2 - \chi_3^2\right) f_2 + \left(\chi_3^2 - \chi_2^2\right) f_1 + \left(\chi_2^2 - \chi_1^2\right) f_3}{2\left(\left(\chi_1 - \chi_3\right) f_2 + \left(\chi_3 - \chi_2\right) f_1 + \left(\chi_2 - \chi_1\right) f_3\right) + \upsilon_0}. \tag{24}$$

where $f(\cdot)$ is the fitness function for CIBAS algorithm, υ_0 is a small positive number.

In Algorithm 1, I_1 is the max iterations for the EKF algorithm, T is the max iterations for QIBAS algorithm, N is dataset size.

Algorithm 1: EKF-QIBAS

Input: I_1, η_0, $\{q_{(i1)}, q_{(i2)}, \ldots, q_{(i6)}\}$, $\{Y_{(1)}, Y_{(2)}, \ldots, Y_{(|N|)}\}$

/--Note: Initialization--/

1 **Initialize:** I_1, T
2 **Initialize:** $\eta=\eta_0$ — T_1
3 **Initialize:** m_0, δ_0, μ, τ

/--Note: Training Starts--/

/--Note: *EKF*-Step--/

4 **for** k=1 **to** $|I_1|$
5 **set** $P_{(0)k}$ random number
6 **set** $K_{(0)k}$ zeros
7 **for** i=1 **to** $|N|$
8 **set** Q_k known
9 **set** R_k known
10 Calculate $\eta_{k|k-1}$ based on (7)
11 Computing H_k with (4) — T_2
12 Calculating $P_{k|k-1}$ with (8)
13 Updating K_k with (9)
14 Computing $\eta_{k|k}$ with (10)
15 Computing $P_{k|k}$ based on (11)
16 **end for**
17 **end for**

18 $\eta_{ekf}=\eta_{k|k}$

/--Note: *QIBAS*-Step--/

19 **for** t=1 **to** $|T|$
20 **set** $\eta^0=\eta_{ekf}$
21 **set** $\eta_{best}=\eta^0$
22 **set** $f_{best}=f(\eta^0)$
23 **for** i=1 **to** $|N|$
24 Updating $\boldsymbol{b}$ with (14) — T_3
25 Computing η_{rt} and η_{lt} with (15)
26 Calculate $f(\eta_{rt})$ and $f(\eta_{lt})$ with (5)
27 Compute η_{t+1} with (17)
28 Computing $f(\eta_{t+1})$ based on (5)
29 Update η_{tk} with (21)
30 Computing $f(\eta_{tk})$ based on (5)
31 **end for**
32 **if** $f(\eta_{tk})<f(\eta_{t+1})$ then
33 $f(\eta_{t+1})=f(\eta_{tk})$, $\eta_{t+1}=\eta_{tk}$
34 **end if**
35 **if** $f(\eta_{t+1})<f(\eta_{best})$ then
36 $f(\eta_{best})=f(\eta_{t+1})$, $\eta_{best}=\eta_{t+1}$
37 **end if**
38 Calculating δ_{t+1}, m_{t+1} with (16)
39 **end for**

/--Note: Training Ends--/

Output: η_{best}, $f(\eta_{best})$

IV. Experimental Results

A. General Settings

1) Evaluation Metrics: The root mean squared error (RMSE), standard deviation (STD) and the maximum error (MAX) are used as the accuracy evaluation metrics [20-25]. They can be described as follow:

$$MAX = \max\left\{\sqrt{\left(Y_i - Y_i'\right)^2}\right\}, i = 1, 2, \cdots n,$$
$$STD = \frac{1}{n}\sum_{i=1}^{n}\sqrt{\left(Y_i - Y_i'\right)^2}, \quad (25)$$
$$RMSE = \sqrt{\frac{1}{n}\sum_{i=1}^{n}\left(Y_i - Y_i'\right)^2}.$$

[1] https://github.com/Lizhibing1490183152/RobotCali.

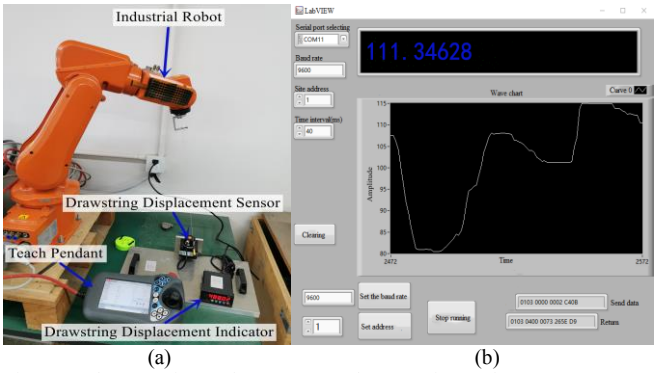

(a) (b)

Fig. 2. The experimental scene. (a) The experimental system: an ABB IRB120 robot, a drawstring displacement sensor, a drawstring displacement indicator and RS485 communication module. (b) The data collection software.

2) Datasets: Four public available robot datasets are collected from website in our experiments. Their details are as follow:

a) **D1: RobotCali-1**. Firstly, 2,000 measuring points on an ABB IRB 120 industrial robot are collected by using a drawstring displacement sensor. Then we select 120 measuring points from this dataset to conduct the experiments. In addition, the experimental scene is shown in Fig. 2. Moreover, detailed information about the collected dataset is publicly available[1].
b) **D2: RobotCali-2**. Similar to dataset D1, we also select other 100 measuring points on the same ABB IRB 120 industrial robot.
c) **D3: The robot accuracy dataset [7]**, which is collected on an UR10 CB3 Robot. It has four datasets: Series A, B, C and D, which has 16,811 samples. Moreover, 200 samples from Series A are selected to conduct our experiments.
d) **D4: HSR-RobotCali [25]**, which has collected 2,000 measuring points on a HSR JR680 industrial robot. Moreover, we select 120 samples for conducting the experiments.

For each dataset, the 80%-20% train–test setting is adopted to obtain the objective results.

B. Experimental Performance

1) Compared algorithms

In this part, the experimental results of several advanced robot calibration algorithms is compared against our developed algorithm. Their details are as follow:

a) **M1: Extended Kalman filter algorithm (EKF)** [5], which can also suppress the non-Gaussian noises.
b) **M2: Beetle antennae search algorithm (BAS)** [11], which has the fast convergence rate and simple principle.
c) **M3: Unscented Kalman filter algorithm (UKF)** [13], which can address noises in robot calibration.
d) **M4: Particle swarm optimization algorithm (PSO)** [14], which is also adopted for searching optimal parameters.
e) **M5: Radial basis function neural network (RBF)** [15], which can estimate the positional error of target position.

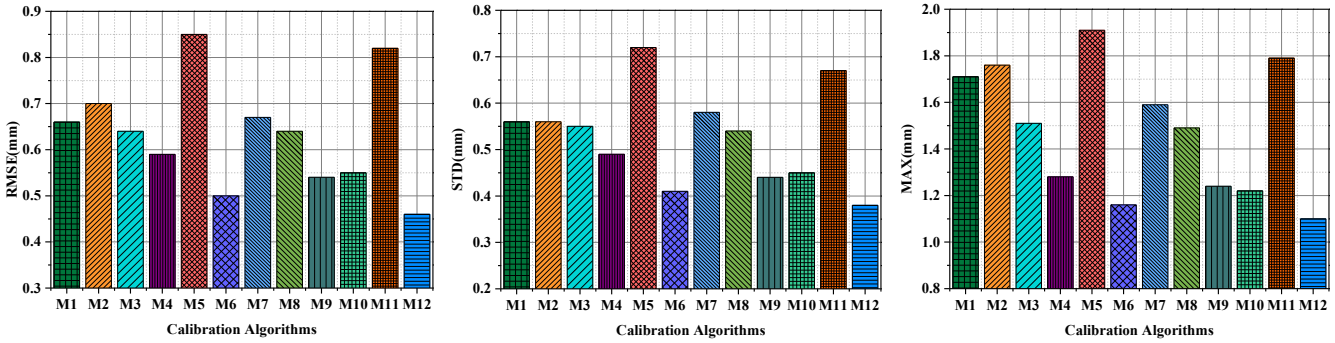

(a)RMSE (b) Error STD (c) Maximum Error

Fig. 3. Robot calibration results of M1-M12 on D1.

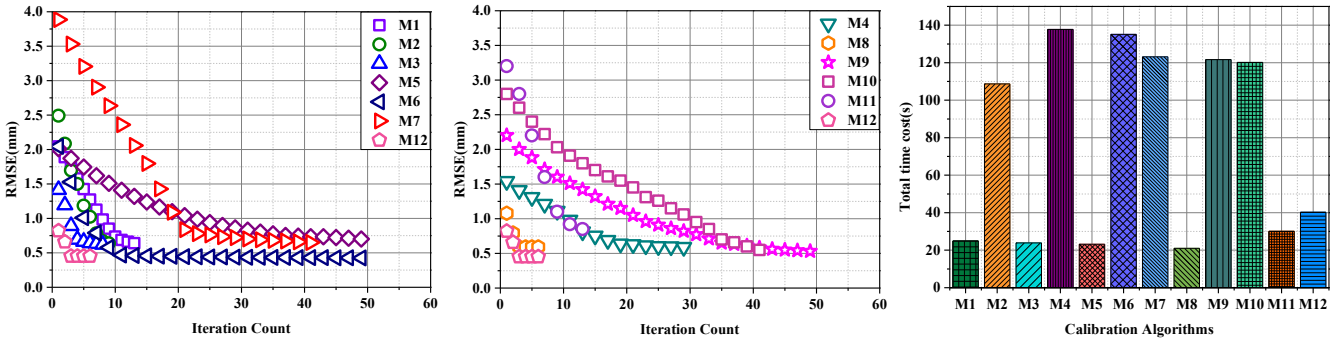

(a) M1-3, M5-7 and M12 (b) M4 and M8-12 (c) Total time cost of M1-M12

Fig. 4. Training curves and total time cost of these methods on D1.

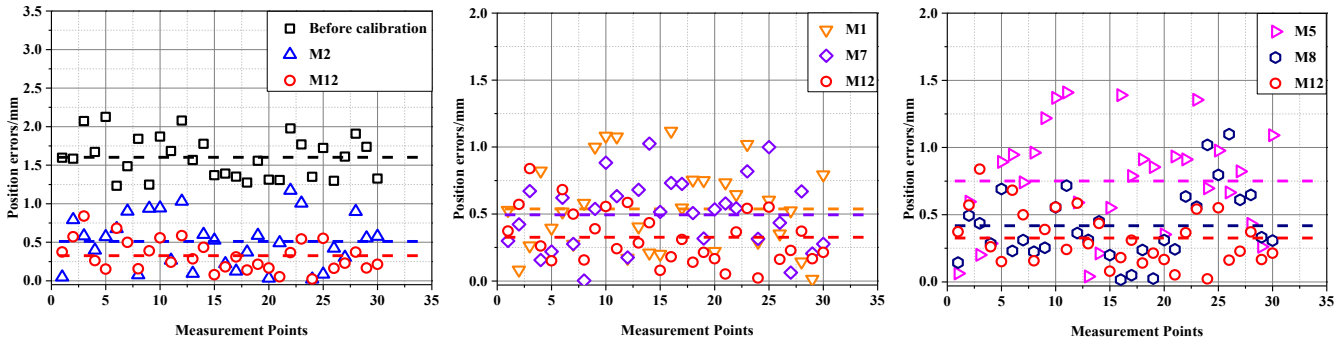

(a) (b) (c)

Fig. 5. The calibration errors through methods on D1. (a) Robot position error of before calibration, M2, M12. (b) Position error of M1, M7, M12. (c) Position error of M5, M8, M12. Moreover, the dotted lines are the average value of these algorithms, M12 has a higher calibration accuracy than its peers do.

f) **M6: Levenberg-Marquardt algorithm (LM)** [6], which has the virtues of both gradient method and Newton method.
g) **M7: Differential evolution algorithm (DE)** [17], which is proposed on the basis of the genetic algorithm.
h) **M8: QIBAS algorithm**, which greatly improves the global convergence ability of BAS algorithm.
i) **M9: Genetic algorithm (GA)** [8].
j) **M10: Simulate anneal algorithm (SA)** [9].
k) **M11: Particle filter (PF)** [4].
l) **M12: EKF-QIBAS algorithm**.

2) Experimental Results of Various Algorithm s

In this work, we make enough comparisons with several state-of-the-art calibration algorithms to explain the correctness of the developed algorithm. Table II shows the RMSE, STD and MAX of these calibration algorithms, Table III records the total time cost of M1-M12. The calibration results through these algorithms on D1 are depicted in Figs. 3, 5. Moreover, Fig. 4 depicts their training curves and total time costs on D1. Based on experiments, we have some findings:

a) **The proposed EKF-QIBAS algorithm achieves higher calibration accuracy than compared algorithms.** From Fig.3 and Table II, M12 achieves the MAX at 1.09mm, which is 6.84% lower than M6's 1.77mm. Similar phenomenon can be found on D1-4 when adopting STD and RMSE as the evaluation metrics.
b) **Incorporating quadratic interpolation into the learning rule of a BAS algorithm can greatly improve its convergence rate.** As depicted in Fig. 4(a), (b) and Table III, M8 and M12 take two iterations to converge in RMSE on D1. However, the most fast algorithm M2 takes seven iterations to converge in RMSE on D1. Similar situations are also encountered on D2-4.

TABLE II
THE CALIBRATION RESULTS OF VARIOUS ALGORITHMS.

Dataset	Metric(mm)	Before	M1	M2	M3	M4	M5	M6	M7	M8	M9	M10	M11	M12
D1	RMSE	2.10	0.66	0.70	0.64	0.59	0.85	0.51	0.67	0.64	0.54	0.55	0.82	**0.47**
	STD	2.01	0.56	0.56	0.55	0.49	0.72	0.42	0.58	0.54	0.44	0.45	0.67	**0.37**
	MAX	3.38	1.71	1.76	1.51	1.28	1.91	1.17	1.59	1.49	1.24	1.22	1.79	**1.09**
D2	RMSE	1.72	0.69	0.64	0.58	0.46	0.78	0.44	0.64	0.51	0.47	0.44	0.82	**0.42**
	STD	1.61	0.52	0.50	0.45	0.36	0.63	0.35	0.52	0.38	0.36	0.33	0.68	**0.35**
	MAX	3.73	2.31	2.37	1.83	1.48	2.74	1.41	1.88	1.75	1.52	1.53	2.32	**1.32**
D3	RMSE	2.72	1.31	0.62	1.63	0.98	1.36	0.51	1.56	0.65	0.63	0.68	1.91	**0.44**
	STD	2.71	1.28	0.57	1.62	0.95	1.28	0.50	1.54	0.58	0.52	0.63	1.90	**0.41**
	MAX	3.08	2.32	1.59	1.96	1.46	2.45	0.88	2.27	1.47	1.53	1.64	2.36	**0.83**
D4	RMSE	5.81	1.32	1.45	1.26	1.05	1.56	0.98	1.22	0.95	1.24	1.15	1.24	**0.78**
	STD	5.76	1.25	1.41	1.23	1.01	1.54	0.95	1.19	0.89	1.17	1.11	1.22	**0.75**
	MAX	6.84	1.64	1.75	1.55	1.32	1.95	1.27	1.58	1.16	1.58	1.46	1.62	**0.92**

TABLE III
TIME COST OF M1-M12 ON RMSE.

Dataset	Item	M1	M2	M3	M4	M5	M6	M7	M8	M9	M10	M11	M12
D1	Iteration	13	7	8	30	400	60	40	2	50	40	12	**2**
	Time(s)	24.66	108.19	23.25	137.36	24.81	135.23	123.56	21.24	121.33	120.35	30.22	**40.64**
D2	Iteration	10	6	8	30	400	55	40	2	50	40	15	**2**
	Time(s)	22.35	101.68	22.35	132.58	22.48	125.15	115.46	20.31	115.69	110.62	29.46	**38.15**
D3	Iteration	14	20	12	50	250	50	50	10	45	45	12	**2**
	Time(s)	70.23	141.43	108.45	438.44	117.78	220.81	220.35	43.66	458.56	421.87	45.92	**111.48**
D4	Iteration	12	8	9	30	400	60	45	2	55	45	13	**2**
	Time(s)	25.56	110.23	28.36	142.39	26.49	148.21	132.65	22.58	130.68	118.34	28.56	**45.92**

TABLE IV
THE CALIBRATED RESULTS OF KINEMATIC PARAMETERS.

Joint i	α_i/°	a_i/mm	d_i/mm	θ_i/°
1	-89.9345	0.3579	289.2391	-0.4892
2	-0.0345	268.3468	3.6792	-89.6092
3	-89.6792	69.1437	0.3891	0.3491
4	90.1356	-2.9864	302.9803	0.3846
5	-90.5681	-1.3692	-0.8531	0.0852
6	0.3469	-1.2891	72.7831	0.2569

c) **The developed QIBAS algorithm can effectively reduce iteration time cost of a BAS algorithm.** From Fig. 4(c) and Table III, M8 takes 21.24s converge in RMSE on D1, which is 80.37% lower than M2's 108.19s. Similar results can be obtained on D2-4. To enhance the robot calibration accuracy of QIBAS algorithm, we adopt the EKF algorithm to deal with the non-Gaussian noises in calibration process. However, the EKF-QIBAS algorithm suffers from loss of computational efficiency. We will design an model parallelization with the help of GPU or other parallelization computing frameworks for addressing this issue.

d) **The proposed EKF-QIBAS algorithm has the lowest robot positioning error among M1-11**. As depicted in Fig. 5, we make extensive comparisons against state-of-the-art algorithms on the calibrated robot positioning error. From the above experimental results, the robot positioning error is significantly reduced after calibration. Moreover, we also can achieve the similar results on D2-4. And finally, the calibrated kinematic parameters is listed in Table IV.

C. Summary

According to the experimental results, we can draw the following summaries:

a) The proposed QIBAS algorithm can accelerate the convergence rate of the BAS algorithm.

b) Based on the QIBAS algorithm, the EKF-QIBAS algorithm is proposed in this work, whose calibration accuracy is higher than the advanced algorithms.

V. CONCLUSIONS

To accurately identify the errors of robot kinematic parameters, EKF-QIBAS algorithm is proposed in this work. The EKF algorithm is employed for initial optimization to address the issue of non-Gaussian noises during the calibration process. Then, a QIBAS algorithm is adopted to further calibrate the robot. To our best knowledge, compared with the existing state-of-the-art calibration algorithms, it has much higher calibration accuracy. Furthermore, the future research work is as follows:

a) Although the proposed EKF-QIBAS algorithm has a high calibration accuracy, its calculation efficiency is relatively low. Thus, the training acceleration methods will be researched to accelerate the training process.

b) Non-geometric factors will be taken into account in modeling to obtain more accurate error sources.

c) Dial indicator is also a common measuring device, its cost is comparably low. We plan to develop an industrial robot calibration scheme based on dial indicator for reducing measurement cost.

d) We will develop the robot calibration scheme based on spatial constraints for complex measurement environment, like plane constraints, distance constrains, line constraints and spherical constraints.

REFERENCES

[1] G Luo, L Zou, Z Wang, C Lv, J Ou, Y Huang, "A novel kinematic parameters calibration method for industrial robot based on Levenberg-Marquardt and Differential Evolution hybrid algorithm," *Robot. Comput.-Integr. Manuf.*, vol. 71, pp. 102165, Oct. 2021.

[2] W. Xu, L. Dongsheng and W. Mingming, "Complete calibration of industrial robot with limited parameters and neural network," in *Proc. of the Int. Conf. on Symposium on Robotics and Intelligent Sensors*, Tokyo, Japan, Dec. 2016, pp. 103-108.

[3] H. R. Zhong, C. H. Hu, X. Y. Li, L. Gao, B. Zeng, and H. Z. Dong, "Kinematic calibration method for a two-segment hydraulic leg based on an improved whale swarm algorithm," *Robot. Comput.-Integr. Manuf.*, vol. 59, pp. 361-372, Oct. 2019.

[4] G. L. Du and P. Zhang, "Online serial manipulator calibration based on multisensory process via extended Kalman and particle filters," *IEEE Trans. Ind. Electron*., vol. 61, no.12, pp.6852-6859, Dec. 2014.

[5] Z. H. Jiang, W. G. Zhou, H. Li, Y. Mo, W. C. Ni, and Q. Huang, "A new kind of accurate calibration method for robotic kinematic parameters based on the extended Kalman and particle filter algorithm," *IEEE Trans. Ind. Electron.*, vol. 65, no. 4, pp. 3337-3345, Apr. 2018.

[6] Y. H. Gan, J. Duan, and X. Z. Dai, "A calibration method of robot kinematic parameters by drawstring displacement sensor," *Int. J. Adv. Robot. Syst*., vol.16, no.5, pp.1-9, Sep.-Oc. 2019.

[7] C. Landgraf, K. Ernst, G. Schleth, M. Fabritius and M. F. Huber, "A hybrid neural network approach for increasing the absolute accuracy of industrial robots," in *Proc. of 2021 IEEE 17th International Conference on Automation Science and Engineering*, Lyon, France, Aug. 2021, pp. 468-474.

[8] C. Fan, G. Zhao, J. Zhao, L. Zhang, L. Sun, "Calibration of a parallel mechanism in a serial-parallel polishing machine tool based on genetic algorithm," *Int. J. Adv. Manuf. Technol,* vol. 81, no.1, pp.27–37, May. 2015.

[9] T. Messay, R. Ordóñez, and E. Marcil, "Computationally efficient and robust kinematic calibration methodologies and their application to industrial robots," *Robotics and Computer-Integrated Manufacturing,* vol. 37, pp. 33-48, Feb. 2016.

[10] Jiang. X, Li. S, "BAS: Beetle antennae search algorithm for optimization problems," *International Journal of Robotics & Control*, vol. 1, no.1, pp. 1-3, Jul. 2018.

[11] Y. X. Wang, Z. W. Chen, H. F. Zu, X. Zhang, C. T. Mao, and Z. R. Wang, "Improvement of heavy load robot positioning accuracy by combining a model-based identification for geometric parameters and an optimized neural network for the compensation of nongeometric errors," *Complexity*, vol. 2020, Article ID 5896813, Jan. 2020.

[12] X. Luo, MC. Zhou, S. Li, *et al*., "Incorporation of efficient second-order solvers into latent factor models for accurate prediction of missing QoS data," *IEEE Trans. Cybernetics*, vol. 48, no. 4, pp. 1216-1228, Apr. 2018.

[13] G. Du, Y. Liang, C. Li, P. X. Liu and D. Li, "Online robot kinematic calibration using hybrid filter with multiple sensors," *IEEE Trans. Instrum. Meas.,* vol. 69, no. 9, pp. 7092-7107, Sept. 2020.

[14] J. H. Lee, J. Song, D. Kim, J. Kim, Y. Kim and S. Jung, "Particle swarm optimization algorithm with intelligent particle number control for optimal design of electric machines," *IEEE Trans. Ind. Electron.*, vol. 65, no. 2, pp. 1791-1798, Feb. 2018.

[15] D. Chen, T. M. Wang, P. J. Yuan, et al., "A positional error compensation method for industrial robots combining error similarity and radial basis function neural network," *Meas. Sci. Technol*., vol. 30, no. 12, pp. 125010, Sep. 2019.

[16] Z. Li, S. Li, and X. Luo, "An overview of calibration technology of industrial robots," *IEEE/CAA J. Autom. Sinica*, vol. 8, no. 1, pp. 23-36, Jan. 2021.

[17] S. Zhou, L. Xing, X. Zheng, N. Du, L. Wang and Q. Zhang, "A self-adaptive differential evolution algorithm for scheduling a single batch-processing machine with arbitrary job sizes and release times," *IEEE Trans. on Cybernetics*, vol. 51, no. 3, pp. 1430-1442, Mar. 2021.

[18] D. Chen, X. Li and S. Li, "A novel convolutional neural network model based on beetle antennae search optimization algorithm for computerized tomography diagnosis," *IEEE Trans. Neural Netw. Learn. Syst.*, DOI: 10.1109/TNNLS.2021.3105384, 2021.

[19] Z. Li, S. Li, O. O. Bamasag, A. Alhothali and X. Luo, "Diversified regularization enhanced training for effective manipulator calibration," *IEEE Trans. Neural Netw. Learn. Syst.*, DOI: 10.1109/TNNLS.2022.3153039.

[20] Z. Li, S. Li, A. Francis and X. Luo, "A novel calibration system for robot arm via an open dataset and a learning perspective," *IEEE Trans. Circuits and Systems II: Express Briefs*, vol. 69, no. 12, pp. 5169-5173, Dec. 2022.

[21] X. Luo, Z. Wang, M. Shang, "An instance-frequency-weighted regularization scheme for non-negative latent factor analysis on high-dimensional and sparse data," *IEEE Trans. on Systems, Man, and Cybernetics: Systems*, vol. 51, no. 6, pp. 3522 - 3532, Jun. 2021.

[22] Y. Jiang, T. Li, L. Wang, F. Chen, "Kinematic accuracy improvement of a novel smart structure-based parallel kinematic machine," *IEEE/ASME Trans. Mechatronics*, vol. 23, no. 1, pp. 469-481, Feb. 2018.

[23] F. Campisano, A. A. Remirez, S. Caló, J. H. Chandler, K. L. Obstein, R. J. Webster, and P. Valdastri, "Online disturbance estimation for improving kinematic accuracy in continuum manipulators," *IEEE robotics and automation letters*, vol. 5, no. 2, pp. 2642-2649, Feb. 2020.

[24] J. He, Q. Y. Ding, F. Gao, and H. B. Zhang, "Kinematic calibration methodology of hybrid manipulator containing parallel topology with main limb," *Measurement*, vol.152, pp.107334, Feb. 2020.

[25] W. Yang, S. Li, Z. Li and X. Luo, "Highly-accurate manipulator calibration via extended Kalman filter-incorporated residual neural network," *IEEE Trans. Industrial Informatics*, DOI: 10.1109/TII.2023.3241614.